

We are IntechOpen, the world's leading publisher of Open Access books Built by scientists, for scientists

6,900

Open access books available

186,000

International authors and editors

200M

Downloads

Our authors are among the

154

Countries delivered to

TOP 1%

most cited scientists

12.2%

Contributors from top 500 universities



WEB OF SCIENCE™

Selection of our books indexed in the Book Citation Index
in Web of Science™ Core Collection (BKCI)

Interested in publishing with us?
Contact book.department@intechopen.com

Numbers displayed above are based on latest data collected.
For more information visit www.intechopen.com



General Adaptive Neighborhood Image Processing for Biomedical Applications

Johan Debayle and Jean-Charles Pinoli
*Ecole Nationale Supérieure des Mines de Saint-Etienne, CIS/LPMG-CNRS
France*

1. Introduction

In biomedical imaging, the image processing techniques using spatially invariant transformations, with fixed operational windows, give efficient and compact computing structures, with the conventional separation between data and operations. Nevertheless, these operators have several strong drawbacks, such as removing significant details, changing some meaningful parts of large objects, and creating artificial patterns. This kind of approaches is generally not sufficiently relevant for helping the biomedical professionals to perform accurate diagnosis and therapy by using image processing techniques. Alternative approaches addressing context-dependent processing have been proposed with the introduction of spatially-adaptive operators (Bouannaya & Schonfeld, 2008; Ciuc et al., 2000; Gordon & Rangayyan, 1984; Maragos & Vachier, 2009; Roerdink, 2009; Salembier, 1992), where the adaptive concept results from the spatial adjustment of the sliding operational window. A spatially-adaptive image processing approach implies that operators will no longer be spatially invariant, but must vary over the whole image with adaptive windows, taking locally into account the image context by involving the geometrical, morphological or radiometric aspects. Nevertheless, most of the adaptive approaches require a priori or extrinsic informations on the image for efficient processing and analysis. An original approach, called General Adaptive Neighborhood Image Processing (GANIP), has been introduced and applied in the past few years by Debayle & Pinoli (2006a;b); Pinoli & Debayle (2007). This approach allows the building of multiscale and spatially adaptive image processing transforms using context-dependent intrinsic operational windows. With the help of a specified analyzing criterion (such as luminance, contrast...) and of the General Linear Image Processing (GLIP) (Oppenheim, 1967; Pinoli, 1997a), such transforms perform a more significant spatial and radiometric analysis. Indeed, they take intrinsically into account the local radiometric, morphological or geometrical characteristics of an image, and are consistent with the physical (transmitted or reflected light or electromagnetic radiation) and/or physiological (human visual perception) settings underlying the image formation processes. The proposed GAN-based transforms are very useful and outperforms several classical or modern techniques (Gonzalez & Woods, 2008) - such as linear spatial transforms, frequency noise filtering, anisotropic diffusion, thresholding, region-based transforms - used for image filtering and segmentation (Debayle & Pinoli, 2006b; 2009a; Pinoli & Debayle, 2007). This book chapter aims to first expose the fundamentals of the GANIP approach (Section 2) by introducing the GLIP frameworks, the General Adaptive Neighborhood (GAN) sets and two

kinds of GAN-based image transforms: the GAN morphological filters and the GAN Choquet filters. Thereafter in Section 3, several GANIP processes are illustrated in the fields of image restoration, image enhancement and image segmentation on practical biomedical application examples. Finally, Section 4 gives some conclusions and prospects of the proposed GANIP approach.

2. Fundamentals of the General Adaptive Neighborhood Image Processing (GANIP) approach

2.1 GLIP frameworks

In order to develop powerful image processing operators, it is necessary to represent intensity images within mathematical frameworks (most of the time of a vectorial nature) based on a physically and/or psychophysically relevant image formation process. In addition, their mathematical structures and operations (the vector addition and then the scalar multiplication) have to be consistent with the physical nature of the images and/or the human visual system, and computationally effective. Thus, although the Classical Linear Image Processing Framework (CLIP), based on the usual vectorial operations, has played a central role in image processing, it is not necessarily the best choice. Indeed, it was claimed (Rosenfeld, 1969) that the usual addition is not a satisfactory solution in some non-linear physical settings, such as that based on multiplicative or convolutive image formation model (Oppenheim, 1967; Stockham, 1972). The reasons are that the classical addition operation and consequently the usual scalar multiplication are not consistent with the combination and amplification laws to which such physical settings obey. However, using the power of abstract linear algebra, it is possible to go up to the abstract level and to explore General Linear Image Processing (GLIP) frameworks (Oppenheim, 1967; Pinoli, 1997a), in order to include situations in which images are combined by processes other than the usual vector addition. Consequently, operators based on such intensity-based image processing frameworks should be consistent with the physical and/or physiological settings of the images to be processed. For instance, the Logarithmic Image Processing (LIP) framework of intensity images (f, g, \dots) has been introduced (Jourlin & Pinoli, 1988; 2001; Pinoli, 1987) with its vector addition \triangle and its scalar multiplication α defined respectively as following:

$$f \triangle g = f + g - \frac{fg}{M} \quad (1)$$

$$\alpha \triangle f = M - M \left(1 - \frac{f}{M} \right)^\alpha, \quad \alpha \in \mathbb{R} \quad (2)$$

where $M \in \mathbb{R}^+$ denotes the upper bound of the range where intensity images are valued.

The LIP framework has been proved to be consistent with the transmittance image formation model, the multiplicative reflectance image formation model, the multiplicative transmittance image formation model, and with several laws and characteristics of human brightness perception (Pinoli, 1997a;b). For example, the figure 1 shows an illustration of X-ray image enhancement in the CLIP and LIP frameworks.

2.2 GAN sets

The space of image (resp. criterion) mappings, defined on the spatial support $D \subseteq \mathbb{R}^2$ and valued in a real numbers interval \tilde{E} (resp. E), is represented in a GLIP framework, denoted \mathcal{I} (resp. \mathcal{C}). The GLIP framework \mathcal{I} (resp. \mathcal{C}) is then supplied with an ordered vectorial

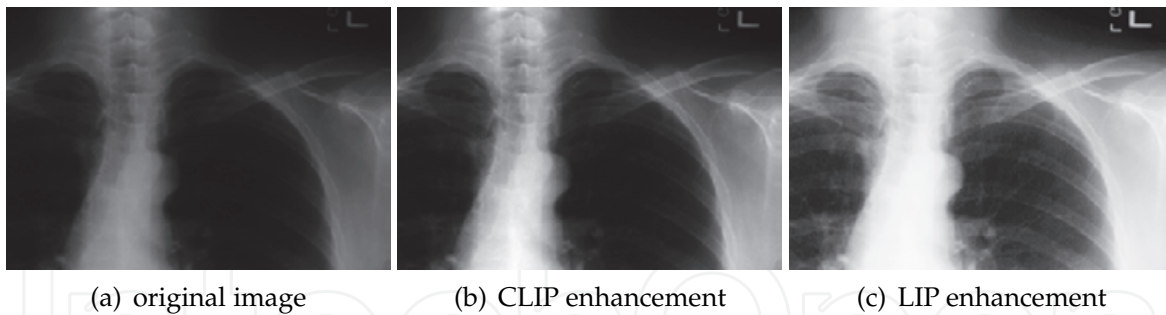


Fig. 1. Example of thorax X-ray image enhancement in the CLIP and LIP frameworks. The LIP framework provides the best results from a visual point of view.

structure, using the formal vector addition \oplus (resp. \otimes), the formal scalar multiplication \otimes (resp. \oplus) and the classical partial order relation \geq defined directly from those of real numbers. Two kinds of General Adaptive Neighborhoods can be introduced: the weak GANs and the strong GANs, defined in the following.

2.2.1 Weak GANs

For each pixel $x \in D$ and for an image $f \in \mathcal{I}$, its associated weak GAN, denoted $V_{m_{\square}}^h(x)$, is included as subset in D . The GANs are built upon a criterion mapping $h \in \mathcal{C}$ (based on a local measurement such as luminance, contrast, thickness, ... related to f), in relation with an homogeneity tolerance m_{\square} belonging to the positive intensity value range E^{\oplus} . The weak GANs are mathematically defined as following:

$$\forall(m_{\square}, h, x) \in E^{\oplus} \times \mathcal{C} \times D, \quad V_{m_{\square}}^h(x) = C_{h^{-1}([h(x) \oplus m_{\square}, h(x) \oplus m_{\square}])(x)} \quad (3)$$

where $C_X(x)$ denotes the path-connected component (with the usual Euclidean topology on $D \subseteq \mathbb{R}^2$) of the subset $X \subseteq D$ containing $x \in D$ and $h^{-1}(Y) = \{x \in D; h(x) \in Y\}$ for $Y \subseteq E$. The weak GANs satisfy several properties (Debayle & Pinoli, 2006a) such as reflexivity, increasing with respect to m_{\square} , equality between iso-valued points, \oplus -translation invariance and \otimes -multiplication compatibility.

To much more understand the definition of the weak GANs, a one-dimensional example is presented in Figure 2, with the CLIP framework selected for the space of criterion mappings. Figure 3 illustrates on a real human retina image the GANs of two pixels computed with the luminance criterion in the CLIP framework with the homogeneity tolerance value $m = 20$. The GANs are self-determined and fit with the local spatial structures of the image. Indeed, the GAN of the pixel within a retinal vessel is only made up of a part of the vascular tree while the other GAN is restricted to the retinal fovea.

2.2.2 Strong GANs

A new collection of GANs, namely the strong GANs, denoted $N_{m_{\square}}^h(x)$, is introduced:

$$\forall(m_{\square}, h, x) \in E^{\oplus} \times \mathcal{C} \times D, \quad N_{m_{\square}}^h(x) = \bigcup_{z \in D} \{V_{m_{\square}}^h(z) | x \in V_{m_{\square}}^h(z)\} \quad (4)$$

Obviously :

$$V_{m_{\square}}^h(x) \subseteq N_{m_{\square}}^h(x) \quad (5)$$

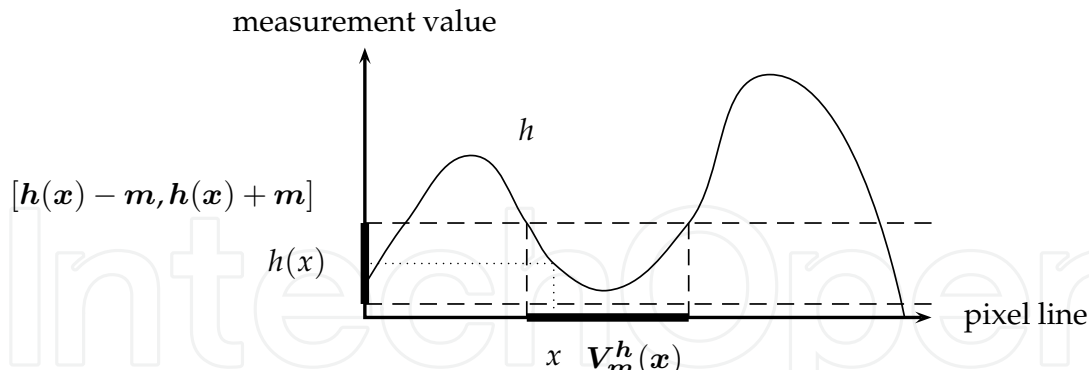


Fig. 2. One-dimensional representation of a weak GAN in the CLIP framework selected for the space of criterion mappings: for a pixel $x \in D$, its associated GAN, $V_m^h(x)$, is computed in relation with the considered criterion mapping $h \in \mathcal{C}$ and a specified homogeneity tolerance value $m \in \mathbb{R}^+$.

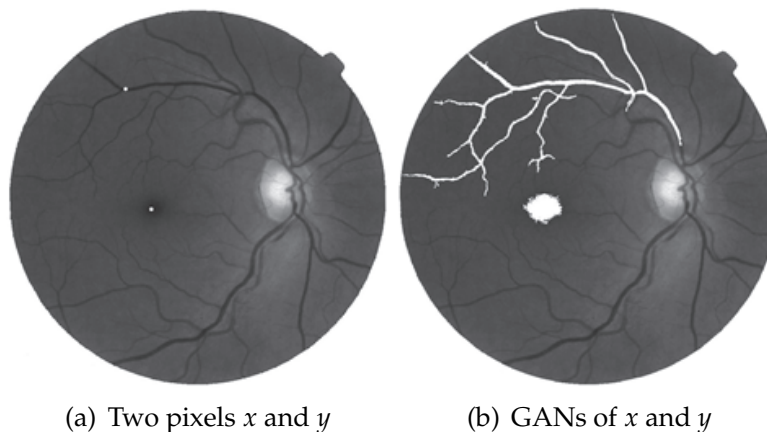


Fig. 3. Example of two weak GANs (b) on a human retina image (a) acquired by optical microscopy. The GANs are determined by the image itself.

The strong GANs $N_{m\Box}^h(x)$ satisfy similar properties as weak GANs. In addition, they satisfy the symmetry property:

$$x \in N_{m\Box}^h(y) \Leftrightarrow y \in N_{m\Box}^h(x) \quad (6)$$

The symmetry condition is relevant for topological and visual reasons (Debayle & Pinoli, 2005b) and allows to simplify the mathematical expressions of adaptive operators without increasing the computational complexity of the algorithms.

These GANs (weak and strong) are now used for defining adaptive morphological and Choquet filters.

2.3 GAN mathematical morphology

The origin of mathematical morphology stems from the study of the geometry of porous media by Matheron (1967). The mathematical analysis is based on set theory and lattice algebra. Its development is characterized by a crossfertilization between applications, methodologies, theories, and algorithms. It leads to several processing tools in the aim

of image filtering, image segmentation, image classification, image measurement, pattern recognition, or texture analysis.

2.3.1 Classical morphological operators

The two fundamental operators of Mathematical Morphology (Serra, 1982) are mappings that commute with the infimum and supremum operations, called respectively erosion and dilation. To each morphological dilation there corresponds a unique morphological erosion, through a duality relation, and vice versa. Two operators ψ and ϕ defines an adjunction or a morphological duality Serra (1982) if and only if: $\forall (f, g) \in \mathcal{I} \quad \psi(f) \leq g \Leftrightarrow f \leq \phi(g)$. The dilation and erosion of an image $f \in \mathcal{I}$ by a Structuring Element (SE) of size r , denoted B_r , are respectively defined as:

$$D_r(f) : \begin{cases} D \rightarrow \tilde{E} \\ x \mapsto \sup_{w \in \check{B}_r(x)} f(w) \end{cases} \tag{7}$$

$$E_r(f) : \begin{cases} D \rightarrow \tilde{E} \\ x \mapsto \inf_{w \in B_r(x)} f(w) \end{cases} \tag{8}$$

where $B_r(x)$ denotes the SE located at pixel x , and $\check{B}_r(x)$ is the reflected subset of $B_r(x)$. The basic idea in the General Adaptive Neighborhood Mathematical Morphology (GANMM) (Debayle & Pinoli, 2006a; Pinoli & Debayle, 2009) is to replace the usual structuring element by GANs, providing adaptive operators and filters.

2.3.2 Adaptive morphological filters

The elementary operators of dilation and erosion use reflected SEs in order to satisfy the morphological adjunction. In order to get this adjunction without considering reflected SEs, the symmetric strong GANs $\{N_{m\ominus}^h(x)\}_{x \in D}$ are used as Adaptive Structuring Elements (ASEs).

The elementary adjunct operators of adaptive dilation and adaptive erosion are defined accordingly to the ASEs:

$$\forall (m_{\ominus}, h, f, x) \in E^{\oplus} \times \mathcal{C} \times \mathcal{I} \times D$$

$$D_{m\ominus}^h(f)(x) = \sup_{w \in N_{m\ominus}^h(x)} f(w) \tag{9}$$

$$E_{m\ominus}^h(f)(x) = \inf_{w \in N_{m\ominus}^h(x)} f(w) \tag{10}$$

Therefore, the most elementary adaptive morphological filters can be defined: the GAN closing and the GAN opening.

$$\forall (m_{\ominus}, h, f) \in E^{\oplus} \times \mathcal{C} \times \mathcal{I}$$

$$C_{m\ominus}^h(f) = E_{m\ominus}^h \circ D_{m\ominus}^h(f) \tag{11}$$

$$O_{m\ominus}^h(f) = D_{m\ominus}^h \circ E_{m\ominus}^h(f) \tag{12}$$

In the case where luminance is selected for the analyzing criterion ($h \equiv f$), these adaptive morphological filters are connected operators (for all (x, y) neighboring points - with the usual Euclidean topology on $D \subseteq \mathbb{R}^2$ - if $h(x) = h(y)$ then $N_{m\ominus}^h(x) = N_{m\ominus}^h(y)$ and therefore

$D_{m\ominus}^h(x) = D_{m\ominus}^h(y)$, which is an overwhelming advantage compared to the usual ones that fail to this strong property. Therefore, the building by composition or combination with the supremum and the infimum of these filters define connected operators, such as adaptive closing-opening and opening-closing filters:

$$\forall(m\ominus, h, f) \in E^{\ominus} \times \mathcal{C} \times \mathcal{I}$$

$$CO_{m\ominus}^h(f) = C_{m\ominus}^h \circ O_{m\ominus}^h(f) \quad (13)$$

$$OC_{m\ominus}^h(f) = O_{m\ominus}^h \circ C_{m\ominus}^h(f) \quad (14)$$

The example of Fig. 4 illustrates the application of the usual and adaptive morphological operators of dilation and erosion on a human retinal vessels image. The adaptive operators do not damaged the spatial structures contrary to the usual ones.

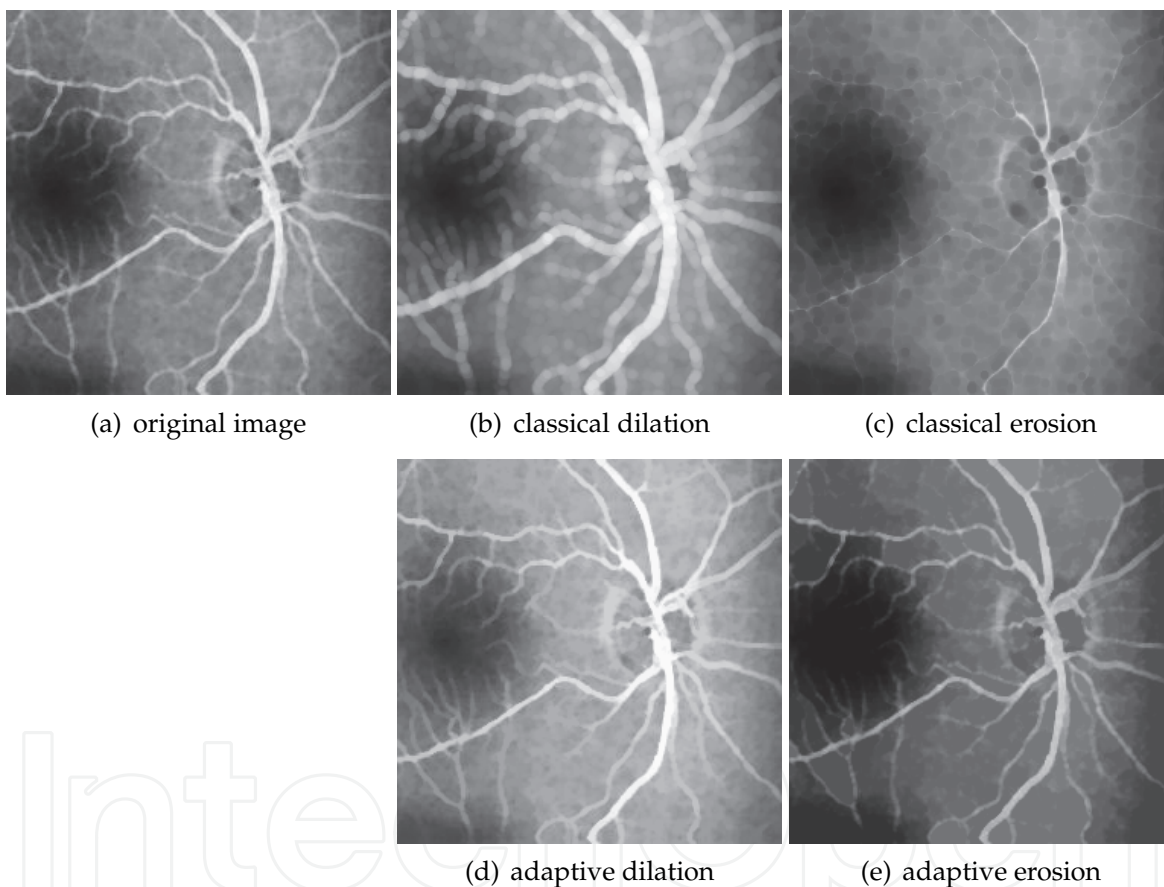


Fig. 4. Original image of human retinal vessels (a). Usual dilation (b) and erosion (c) of the original image using a disk of radius 2 as SE. Adaptive dilation (d) and erosion (e) of the original image using ASEs computed in the CLIP framework on the luminance criterion with the homogeneity tolerance value $m = 15$.

2.3.3 Adaptive sequential morphological filters

The families of adaptive morphological filters $\{O_m^h\}_{m \geq 0}$ and $\{C_m^h\}_{m \geq 0}$ are generally not a size distribution and antisize distribution (Serra, 1982) respectively, since the notion of semi-group is generally not satisfied. This kind of filters is largely used in image processing and analysis.

In the GANIP approach, such families can be built by naturally reiterate adaptive dilations or erosions. Explicitly, adaptive sequential dilation, and erosion are respectively defined as :

$$\forall(m_{\square}, h, f) \in E^{\oplus} \times \mathcal{C} \times \mathcal{I}$$

$$D_{m,p}^h(f) = \underbrace{D_m^h \circ \dots \circ D_m^h}_{p \text{ times}}(f) \tag{15}$$

$$E_{m,p}^h(f) = \underbrace{E_m^h \circ \dots \circ E_m^h}_{p \text{ times}}(f) \tag{16}$$

The morphological adjunction of $D_{m,p}^h$ and $E_{m,p}^h$ provides, among other things, the two following adaptive sequential closing and opening filters:

$$C_{m,p}^h(f) = E_{m,p}^h \circ D_{m,p}^h(f) \tag{17}$$

$$O_{m,p}^h(f) = D_{m,p}^h \circ E_{m,p}^h(f) \tag{18}$$

Moreover, the families $\{O_{m,p}^h\}_{p \geq 0}$ and $\{C_{m,p}^h\}_{p \geq 0}$ generate size and antisize distributions, respectively. The extension to GANMM of the well-known alternating sequential filters (ASFs) can then be defined (Debayle & Pinoli, 2005a):

$$\forall(m, n, h) \in E^{\oplus} \times \mathbb{N} \setminus \{0\} \times \mathcal{C}, \quad \forall(p_i) \in \mathbb{N}^{\llbracket 1, n \rrbracket} \text{ increasing sequence}$$

$$\text{ASFOC}_{m,n}^h(f) = \text{OC}_{m,p_n}^h \circ \dots \circ \text{OC}_{m,p_1}^h(f) \tag{19}$$

$$\text{ASFCA}_{m,n}^h(f) = \text{CO}_{m,p_n}^h \circ \dots \circ \text{CO}_{m,p_1}^h(f) \tag{20}$$

2.3.4 Adaptive toggle contrast filters

The usual toggle contrast filter (Soille, 2003) is an edge sharpness operator. This filter is defined from the classical dilation and erosion using a disk of radius r as structuring element. This (non-adaptive) filter is here defined in the GANIP framework using a local 'contrast' criterion, such as the local contrast defined in Jourlin et al. (1988). The LIP contrast at a pixel $x \in D$ of an image $f \in \mathcal{I}$, denoted $c(f)(x)$, is defined with the help of the gray values of its neighbors included in a disk $V(x)$ of radius 1, centered in x :

$$c(f)(x) = \frac{1}{\#V(x)} \sum_{y \in V(x)} (\max(f(x), f(y)) \Delta \min(f(x), f(y))) \tag{21}$$

where \sum and $\#$ denote the sum in the LIP sense (Jourlin et al., 1988), and the cardinal symbol, respectively. The LIP contrast is here defined in the discrete case, but a continuous definition has been proposed by Pinoli (1991; 1997b). The so-called adaptive toggle contrast filter is the image transformation denoted $\kappa_{m_{\square}}^{c(f)}$, where $c(f)$ and m_{\square} represent the criterion mapping and the homogeneity tolerance within the GLIP framework (required for the GANs definition), respectively. It is defined as following:

$$\forall(f, x, m_{\square}) \in \mathcal{I} \times D \times E^{\oplus}$$

$$\kappa_{m_{\square}}^{c(f)}(f)(x) = \begin{cases} D_{m_{\square}}^{c(f)}(f)(x) & \text{if } D_{m_{\square}}^{c(f)}(f)(x) \ominus f(x) < f(x) \ominus E_{m_{\square}}^{c(f)}(f)(x) \\ E_{m_{\square}}^{c(f)}(f)(x) & \text{otherwise} \end{cases} \tag{22}$$

where $D_{m\ominus}^{c(f)}$ and $E_{m\ominus}^{c(f)}$ denote the adaptive dilation and adaptive erosion computed with the criterion mapping $c(f)$.

More details on the GAN-based morphological filters can be found in Debayle & Pinoli (2006b); Pinoli & Debayle (2009).

2.4 GAN Choquet filtering

Fuzzy integrals (Choquet, 2000; Sugeno, 1974) provide a general representation of image filters. A large class of operators can be represented by those integrals such as linear filters, morphological filters, rank filters, order statistic filters or stack filters (Grabisch, 1994). The main fuzzy integrals are Choquet integral (Choquet, 2000) and Sugeno integral (Sugeno, 1974). Fuzzy integrals integrate a real function with respect to a fuzzy measure.

2.4.1 Fuzzy integrals

Let X be a finite set. In discrete image processing applications, X represents the K pixels within a subset of the spatial support of the image (i.e. an image window). A fuzzy measure over $X = \{x_0, \dots, x_{K-1}\}$ is a function $\mu : 2^X \rightarrow [0, 1]$ such that:

- $\mu(\emptyset) = 0; \mu(X) = 1$
- $\mu(A) \leq \mu(B)$ if $A \subseteq B$

Fuzzy measures are generalizations of probability measures for which the probability of the union of two disjoint events is equal to the sum of the individual probabilities.

The discrete Choquet integral of a function $f : X = \{x_0, \dots, x_{K-1}\} \mapsto \tilde{E}$ with respect to the fuzzy measure μ is (Murofushi & Sugeno, 1989):

$$C_\mu(f) = \sum_{i=0}^{K-1} (f(x_{(i)}) - f(x_{(i-1)}))\mu(A_{(i)}) = \sum_{i=0}^{K-1} (\mu(A_{(i)}) - \mu(A_{(i+1)}))f(x_{(i)}) \quad (23)$$

where the subsymbol $(.)$ indicates that the indices have been permuted so that: $0 = f(x_{(-1)}) \leq f(x_{(0)}) \leq f(x_{(1)}) \leq \dots \leq f(x_{(K-1)})$, $A_{(i)} = \{x_{(i)}, \dots, x_{(K-1)}\}$ and $A_{(K)} = \emptyset$.

An interesting property of the Choquet fuzzy integral is that if μ is a probability measure, the fuzzy integral is equivalent to the classical Lebesgue integral and simply computes the expectation of f with respect to μ within the usual probability framework. The fuzzy integral is a form of averaging operator in the sense that the fuzzy integral is valued between the minimum and maximum values of the function f to be integrated.

2.4.2 Choquet filters

Let f be in \mathcal{I} , W a window of K pixels and μ a fuzzy measure defined on W . This measure could be extended to all translated window W_y associated to a pixel y : $\forall A \subseteq W_y \quad \mu(A) = \mu(A_{-y}), A_{-y} \subseteq W$. In this way, the Choquet filter associated to f is defined by:

$$\forall y \in D, \quad CF_\mu^W(f)(y) = \sum_{x_i \in W_y} (\mu(A_{(i)}) - \mu(A_{(i+1)}))f(x_{(i)}) \quad (24)$$

The Choquet filters generalize (Grabisch, 1994) several classical filters:

- linear filters (mean, Gaussian, ...):
 $LF_W^\alpha(f)(y) = \sum_{x_i \in W_y} \alpha_i f(x_i)$ where $\alpha \in [0, 1]^K, \sum_{i=0}^{K-1} \alpha_i = 1$
- rank filters (median, min, max, ...):
 $RF_W^d(f)(y) = f(x_{(d)})$ where $d \in [0, K-1] \cap \mathbb{N}$

- order filters (n -power, α -trimmed mean, quasi midrange, ...):

$$OF_W^\alpha(f)(y) = \sum_{x_i \in W_y} \alpha_i f(x_{(i)}) \text{ where } \alpha \in [0, 1]^K, \sum_{i=0}^{K-1} \alpha_i = 1$$

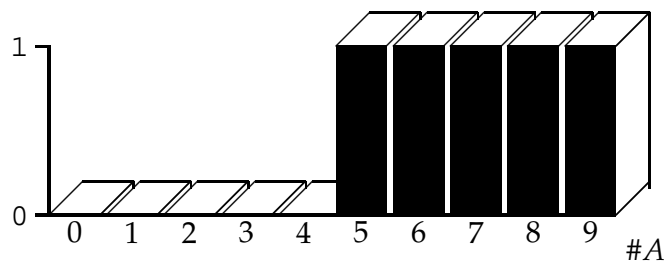
The mean, rank and order filters are Choquet filters with respect to the cardinal measures: $\forall A, B \subseteq W \quad \#A = \#B \Rightarrow \mu(A) = \mu(B)$ ($\#B$ denoting the cardinal of B). Those filters, using an operational window W , could be characterized with the application: $\#A \mapsto \mu(A), A \subseteq W$. Indeed, different cardinal fuzzy measures could be defined for each class of filters:

- mean filter: μ is the fuzzy measure on W defined by $\mu(A) = \#A / \#W$
- rank filters (of order d): μ is the fuzzy measure on W defined by:

$$\mu(A) = \begin{cases} 0 & \text{if } \#A \leq \#W - d \\ 1 & \text{otherwise} \end{cases}$$
- order filters: μ is the fuzzy measure on W defined by: $\mu(A) = \sum_{j=0}^{\#A-1} \alpha_{\#W-j}$

For example, the median filter (using a 3x3 window) is characterized by the following cardinal measure:

$$\forall A \subseteq W \quad \mu(A) = \begin{cases} 0 & \text{if } \#A \leq \lfloor \#W/2 \rfloor \\ 1 & \text{otherwise} \end{cases}$$



where $\lfloor s \rfloor$ denotes the round down of the real number s .

2.4.3 Adaptive Choquet filters

In order to extend Choquet filters with the use of GANs, the neighborhoods $V_m^h(y)$ are used as operational windows W . Since the GANs are spatially-variant, a set of fuzzy measures has to be locally determined: $\{\mu_y : V_m^h(y) \rightarrow [0, 1]\}_{y \in D}$. In this way, the GAN-based Choquet filter is defined as follows:

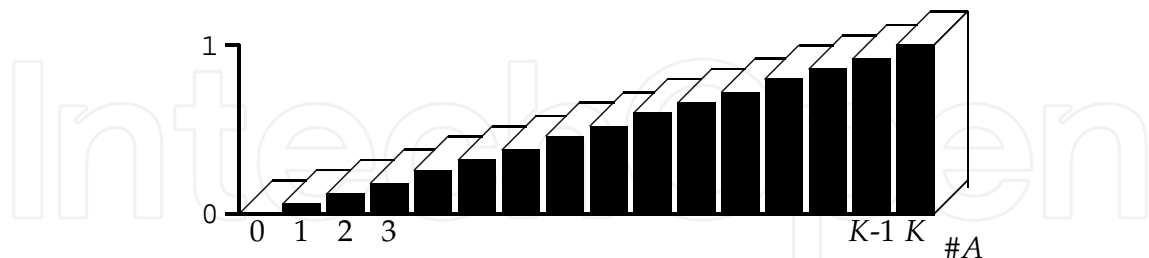
$$\forall (m_\square, h, f, y) \in E^\oplus \times \mathcal{C} \times \mathcal{I} \times D$$

$$CF_{m_\square}^h(f)(y) = \sum_{x_i \in V_m^h(y)} (\mu_y(A_{(i)}) - \mu_y(A_{(i+1)})) f(x_{(i)}) \tag{25}$$

Several filters (Grabisch, 1994), such as the mean filter, the median filter, the min filter, the max filter, the α -trimmed mean filter, the n -power filter, the α -quasi-midrange filter and so on, could consequently be extended to GAN-based Choquet filters (Amattouch, 2005). In the following, a few fuzzy measures μ_y attached to the GAN $V_m^h(y)$ are illustrated with respect to specific GAN-based filters.

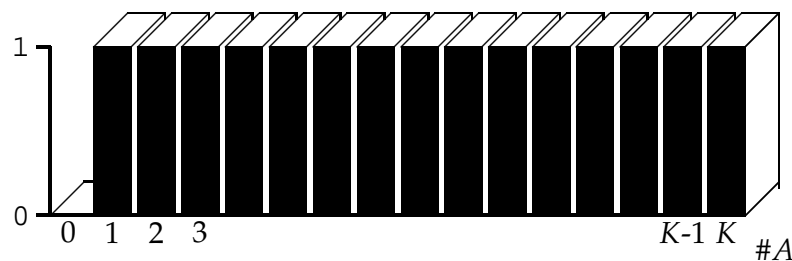
- GAN-based mean filter:

$$\forall A \subseteq V_m^h(y), \quad \mu_y(A) = \frac{\#A}{K}, \text{ where } K = \#V_m^h(y) \tag{26}$$



- GAN-based max filter:

$$\forall A \subseteq V_{m\Box}^h(y), \quad \mu_y(A) = \begin{cases} 0 & \text{if } \#A = 0 \\ 1 & \text{otherwise} \end{cases}, \quad \text{where } K = \#V_{m\Box}^h(y) \quad (27)$$



- GAN-based n -power filter:

$$\forall A \subseteq V_{m\Box}^h(y), \quad \forall n \in [1, +\infty[\quad \mu_y(A) = \left(\frac{\#A}{K}\right)^n, \quad \text{where } K = \#V_{m\Box}^h(y) \quad (28)$$

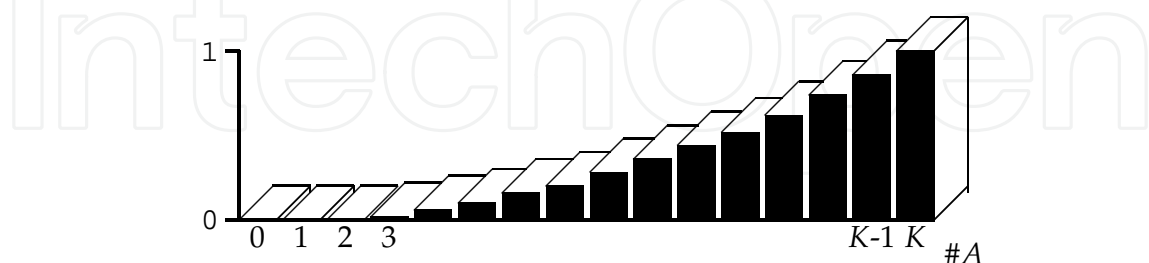


Figure 5 shows an application example, on a magnetic resonance (MR) image of the human brain, of classical Choquet filtering with an operating window W (of size 5×5 pixels) using different fuzzy measures μ corresponding to the max and power filters, respectively.

Those GAN-based Choquet filters provide image processing operators, in a well-defined mathematical framework. More details on these GAN-based Choquet filters can be found in Debayle & Pinoli (2009a;b).

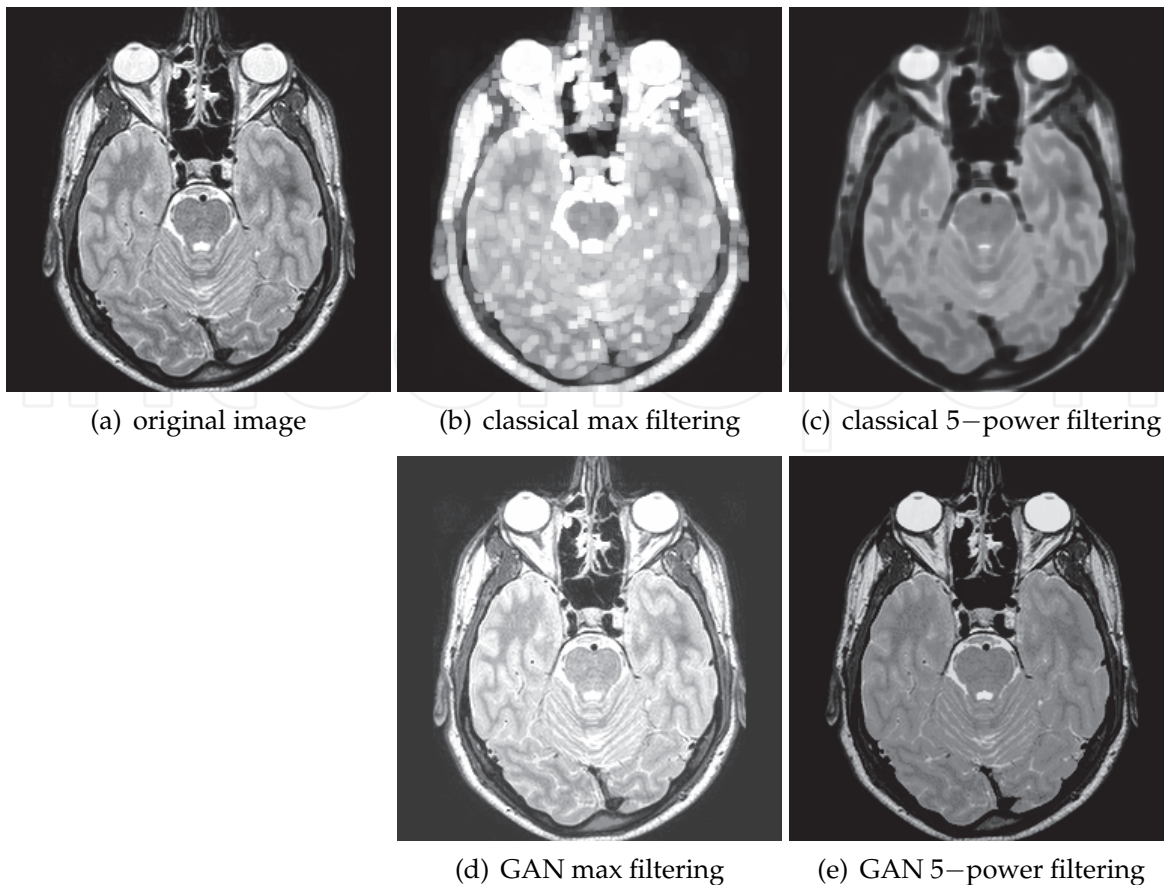


Fig. 5. Classical (b,c) and adaptive Choquet filtering (d,e) of the original brain magnetic resonance (MR) image (a) using different fuzzy measures corresponding to the max filter and the 5–power filter. The classical filters use a 5x5 operating window, while the adaptive filters use GANs computed with the luminance criterion using the homogeneity tolerance value $m = 50$ within the CLIP framework.

3. Biomedical application examples

GANIP-based processes are now exposed and applied in the field of image restoration, image enhancement and image segmentation on practical biomedical application examples.

3.1 Image restoration

The purpose of image restoration is to "compensate for" or "undo" defects which degrade an image. Degradations can come in many forms such as motion blur, noise, and camera misfocus. This restoration process is generally needed before segmenting and analyzing and measuring the regions of interest. In the following, two examples of image restoration are exposed using GAN mathematical morphology and GAN Choquet filtering.

3.1.1 Application to CerebroVascular Accident (CVA) diffusion MR images

This first application example addresses CerebroVascular Accidents (CVA). A stroke or a cerebrovascular accident occurs when the blood supply to the brain is disturbed in some way. As a result, brain cells are starved of oxygen causing some cells to die and leaving other cells damaged. A multiscale restoration of a human brain image f is proposed with a GANIP-based process using adaptive sequential openings $O_{m \square, p}$ (Fig. 6), using the GANs structuring

elements with the luminance criterion mapping f and the homogeneity tolerance $m_{\Delta} = 7$ within the LIP framework. Several levels of decomposition are exposed: $p = 1, 2, 4, 6, 8$ and 10 (see Paragraph 2.3.3). The main aim of this restoration process is to smooth the image background for highlighting the stroke area, in order to help the neurologist for the diagnosis of the kind of stroke, and/or to allow a robust image segmentation to be performed.

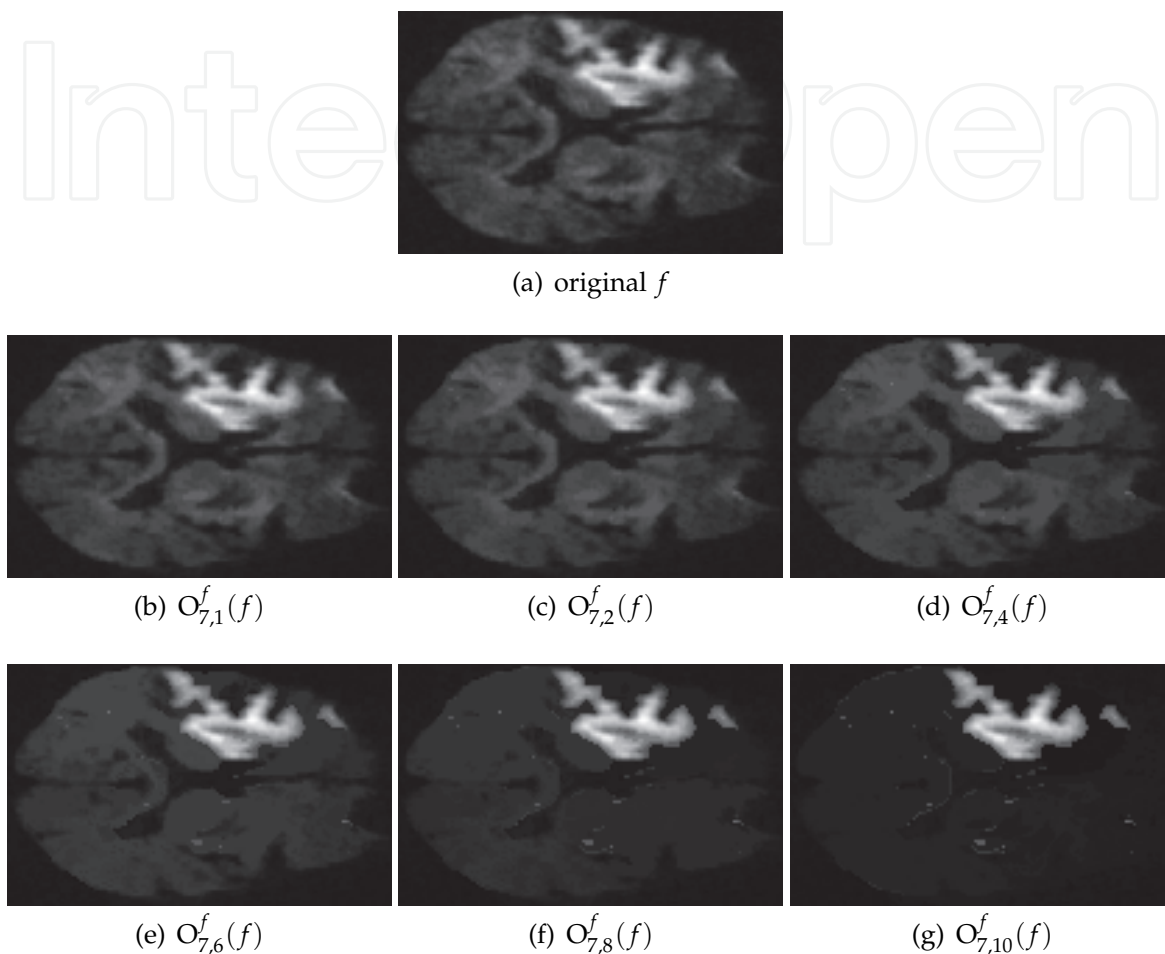


Fig. 6. Image restoration of CerebroVascular Accidents. A multiscale process (b-g) is achieved with the GAN-based morphological sequential openings (within the LIP framework) applied on the original image (a). The detection of the stroke area seems to be reachable at level $p = 10$.

These results show the advantages of spatial adaptivity and intrinsic multiscale analysis of the GANIP-based operators. Moreover, the detection of the stroke area seems to be reachable at level $p = 10$, while accurately preserving both its spatial and intensity characteristics which are needed for a further robust image segmentation.

3.1.2 Application to human brain MR images

This second application example is focused on the restoration of a human brain MR image (Fig. 7). This process is generally required before segmenting the different anatomical structures of the brain. The following GAN mean filter is both performed in the classical and adaptive framework in order to compare the two approaches: The adaptive filtering is

applied with the luminance criterion using the homogeneity tolerance value $m = 30$, while the classical filtering uses a disk of radius 2 as operational window.

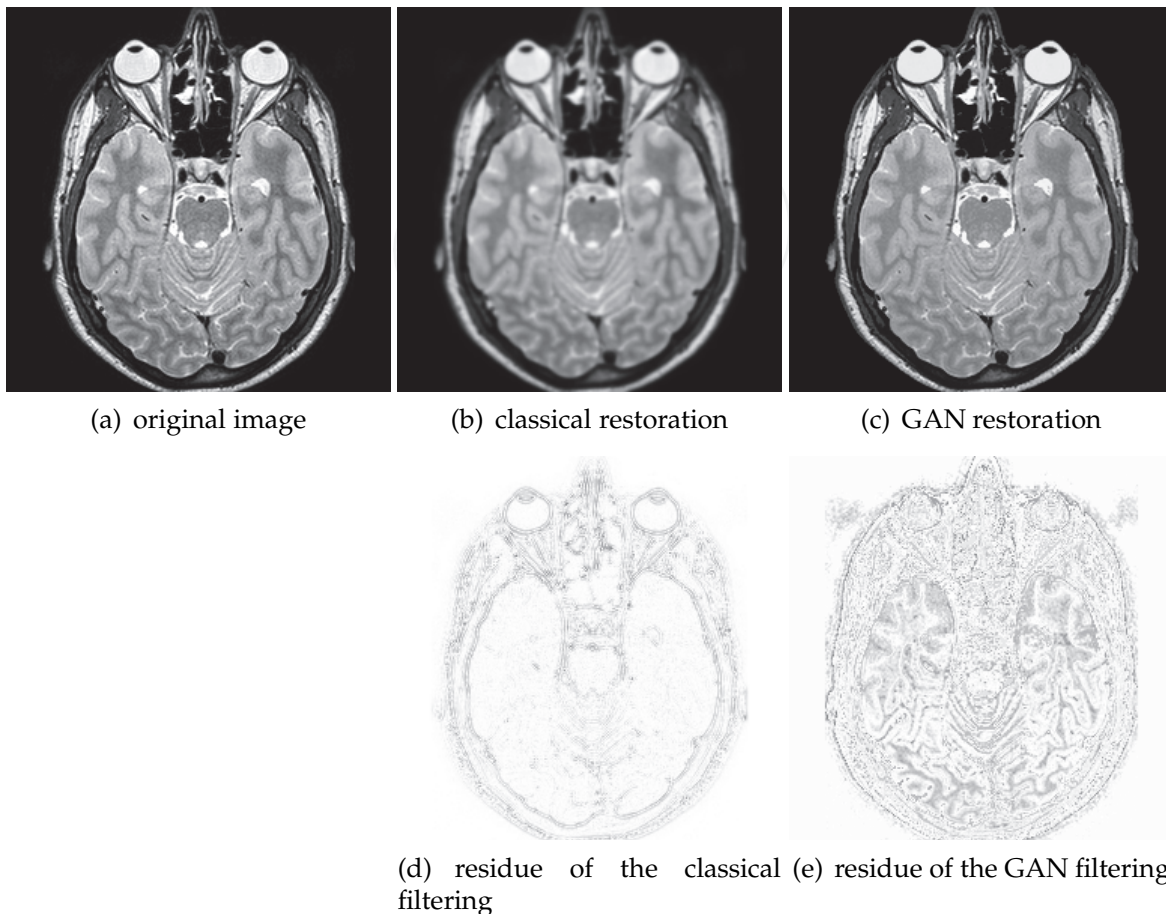


Fig. 7. Image restoration of a MR brain image (a) using a classical Choquet mean filtering (b) (with a disk of radius 2) and a GAN Choquet mean filtering (c) (within the CLIP model using the tolerance value $m = 30$). The residues of the resulting filtered images are shown in (d) and (e) with a gray tone inversion for a better visualization.

This example shows that the GAN filtering smooths the image while preserving spatial and intensity structures. On the contrary, the classical filtering acts on the different gray levels in the same way and consequently damages the region transitions. This difference is clearly shown in the filtering residues. Indeed, in the classical case, only the image transitions are highlighted. Consequently, the classical filtered image is blurred contrary to the adaptive filtered image.

3.2 Image enhancement

Image enhancement is the improvement of image quality (Gonzalez & Woods, 2008), wanted e.g. for visual inspection. Physiological experiments have shown that very small changes in luminance are recognized by the human visual system in regions of continuous gray tones, and not at all seen in regions of some discontinuities (Stockham, 1972). Therefore, a design goal for image enhancement is often to smooth images in more uniform regions, but to preserve edges. On the other hand, it has also been shown that somehow degraded images with enhancement of certain features, e.g. edges, can simplify image interpretation

both for a human observer and for machine recognition (Stockham, 1972). A second design goal, therefore, is image sharpening (Gonzalez & Woods, 2008).

3.2.1 Application to human retina optical images

The following example (Fig. 8) is focused on human retinal vessels. The aim of this application is to highlight the vessels in order to help the ophthalmologists to make a diagnosis. For example, some retinal pathologies affect the tortuosity or the diameter of the blood vessels. The considered image enhancement technique is an edge sharpening process: the approach is similar with unsharp masking (Ramponi et al., 1996) type enhancement where a high pass portion is added to the original image. The contrast enhancement process is here realized through the GAN-based toggle contrast filter (Eq. 22). This adaptive process will be compared with the classical toggle contrast filter, whose operator κ_r is defined as follows (Soille, 2003):

$$\forall (f, x, r) \in I \times D \times \mathbb{R}^+, \quad \kappa_r(f)(x) = \begin{cases} D_r(f)(x) & \text{if } D_r(f)(x) - f(x) < f(x) - E_r(f)(x) \\ E_r(f)(x) & \text{otherwise} \end{cases} \quad (29)$$

where D_r and E_r denote the classical dilation and erosion, respectively, using a disk of radius r as structuring element.

This image enhancement example confirms that the GANIP operators are more effective than the corresponding classical ones. Indeed, the adaptive toggle contrast performs a locally accurate image enhancement, taking into account the notion of homogeneity within the spatial structures of the image. Consequently, only the transitions are sharpened while preserving the homogeneous regions. On the contrary, the usual toggle contrast enhances the image in an uniform way. Thus, the spatial zones around transitions are rapidly damaged as soon as the filtering becomes too strong.

3.2.2 Application to osteoblastic cell fluorescence optical images

A second application example addresses the study of interactions between osteoblastic cells and some biomaterials for biocompatibility purposes which are essential for bone tissue engineering (orthopedic implants). For this application, the biologists study the adhesion of osteoblastic cells of bones with hydroxyapatite-based biomaterials. In this aim, some images of cells are acquired by fluorescence optical microscopy. Unfortunately, the images show a low contrast. In this way, an image enhancement process is proposed using the GAN max Choquet filtering (within the CLIP framework) followed by a stretching of the gray-tone range.

The cells are more and more highlighted according to the homogeneity tolerance value of the GANs. This GAN-based image enhancement is very useful for helping the biologists to identify the cells and characterize its interactions with the biomaterials on such images.

3.3 Image segmentation

The segmentation of an intensity image can be defined as its partition (in fact the partition of the spatial support D) into different connected regions, relating to an homogeneity condition (Gonzalez & Woods, 2008). A common segmentation process is based on a morphological transformation called watershed (Beucher & Lantuejoul, 1979). It will be illustrated on the two following examples.

3.3.1 Application to protein gel electrophoresis optical images

This first application example of image segmentation is focused on the proteomic expression analysis of colorectal cancer by two-dimensional differential gel electrophoresis (2D-DIGE)

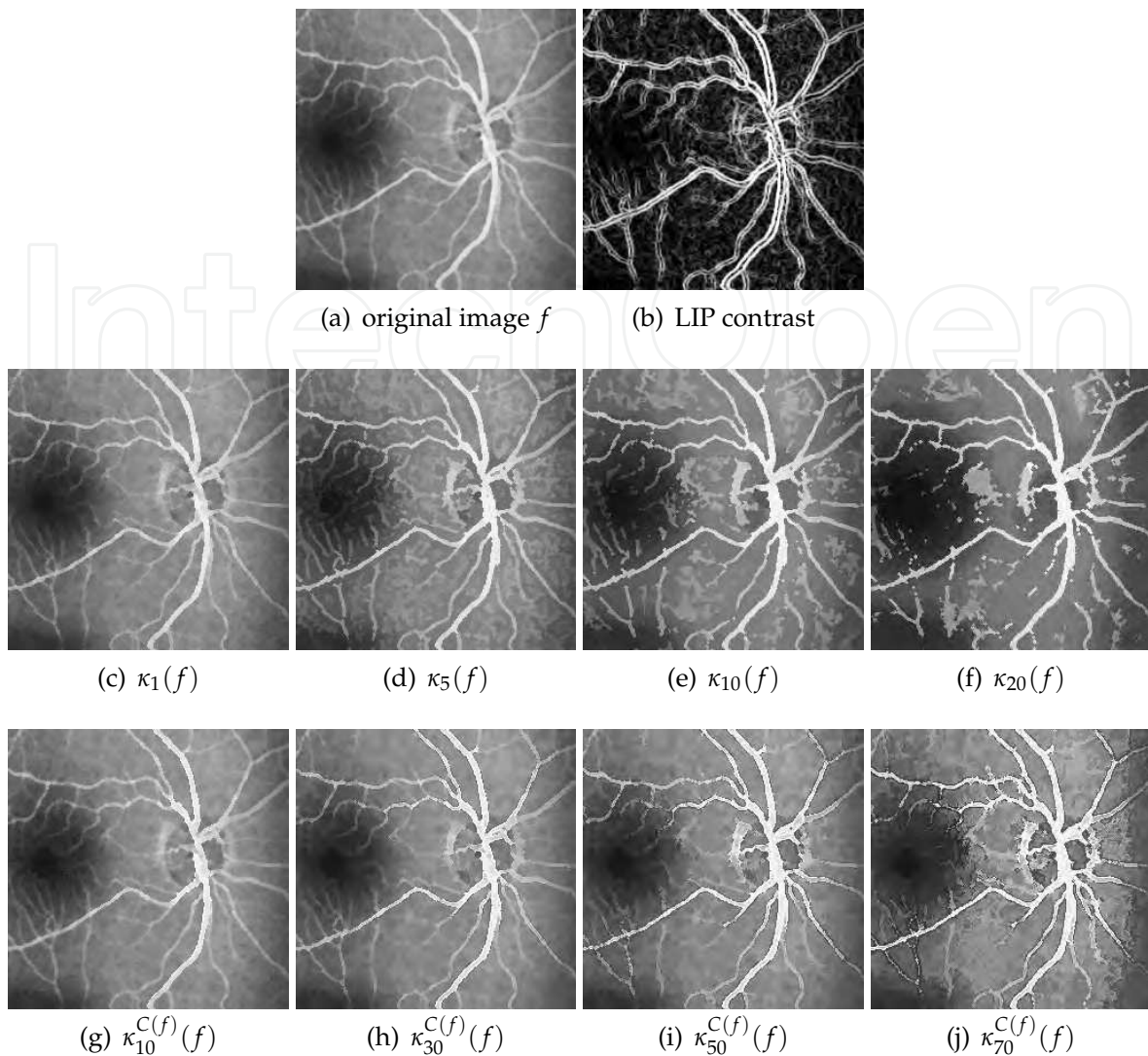


Fig. 8. Image enhancement of human retinal vessels through the toggle contrast process. The operator is applied on a real (a) image acquired on the retina of a human eye. The enhancement is achieved with the usual toggle contrast (c-f) and the GANIP-based toggle contrast (g-j), respectively. Using the usual toggle contrast, the edges are disconnected as soon as the filtering becomes too strong. On the contrary, such structures are preserved and sharpened with the GANIP filters.

(Bernard, 2008). The identification of specific protein markers for colorectal cancer would provide the basis for early diagnosis and detection, as well as clues for understanding the molecular mechanisms governing cancer progression. The objective is to identify the proteins differentially expressed in tumoral and neighboring normal mucosa. For this purpose, a segmentation process using GAN mathematical morphology is performed on 2D-DIGE images (Fig. 10). More precisely, a GAN-based opening-closing is used within the CLIP framework using the homogeneity tolerance value $m = 10$. Thereafter, a constrained watershed process (Soille, 2003) is applied on the filtered image.

The result shows a satisfying segmented image obtained from a very poor contrasted original image. Despite a few errors, the following segmentation process could be used for a specific statistical analysis on a great number of 2D-DIGE images.

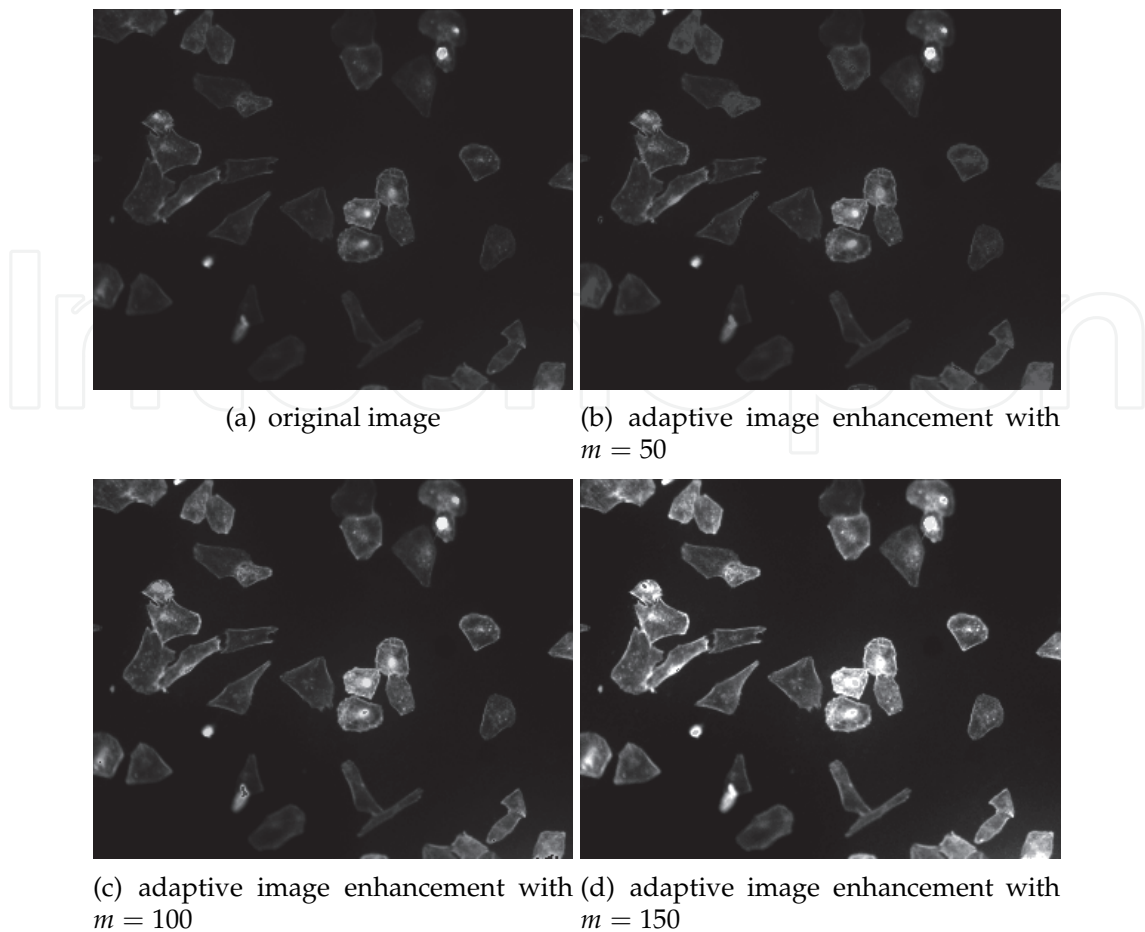


Fig. 9. Image enhancement of osteoblastic cells (a) by a GAN Choquet max filtering in the CLIP model using different homogeneity tolerance values (b-d).

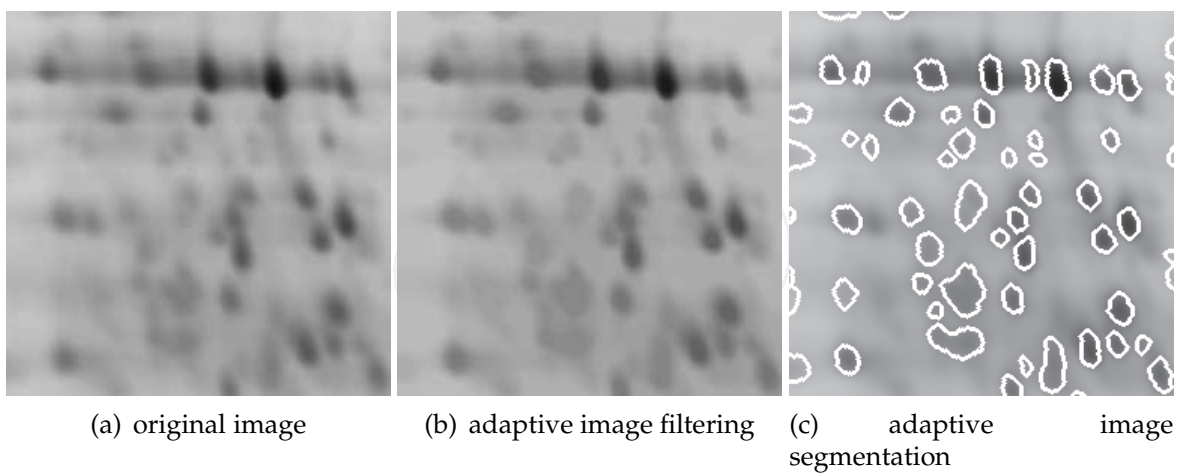


Fig. 10. Image segmentation of a protein gel electrophoresis optical image (a) using a GAN opening-closing filtering (b) followed by a constraint watershed process (c).

3.3.2 Application to human endothelial cornea cell optical images

The second application example is focused on the cornea cell analysis. The cornea is the transparent surface in the front of the eye. It has a role of protection of the eye, and with

the lens, of focusing light into the retina. It is constituted of several layers, such as the epithelium (at the front of the cornea), the stroma and the endothelium (at the back of the cornea). The endothelium contains non-regenerative cells tiled in a monolayer and hexagonal mosaic. This layer pumps water from the cornea, keeping it clear. A high cell density and a regular morphometry of this layer characterize the good quality of a cornea before transplantation, the most common transplantation in the world. Herein lays the importance of the endothelial control. Ex vivo controls are done by optical microscopy on corneal button before grafting. That image acquisition equipment give gray tones images which are segmented (Gavet & Pinoli, 2008), for example by the SAMBA™ software (Gain et al., 2002), into regions representing cells. These ones are used to compute statistics in order to quantify the corneal quality before transplantation.

The authors proposed a GANIP-based approach to segment the cornea cells. The process is achieved by a closing-opening morphological filtering using the GAN sets with the luminance criterion in the CLIP framework, followed by a watershed transformation. A comparison with the results provided by the SAMBA™ software, whose process is achieved by thresholding, filtering and skeletonization (Gain et al., 2002), is proposed (Fig. 11). The parameter m of the adaptive morphological filter has been tuned to visually provide the best possible segmentation.

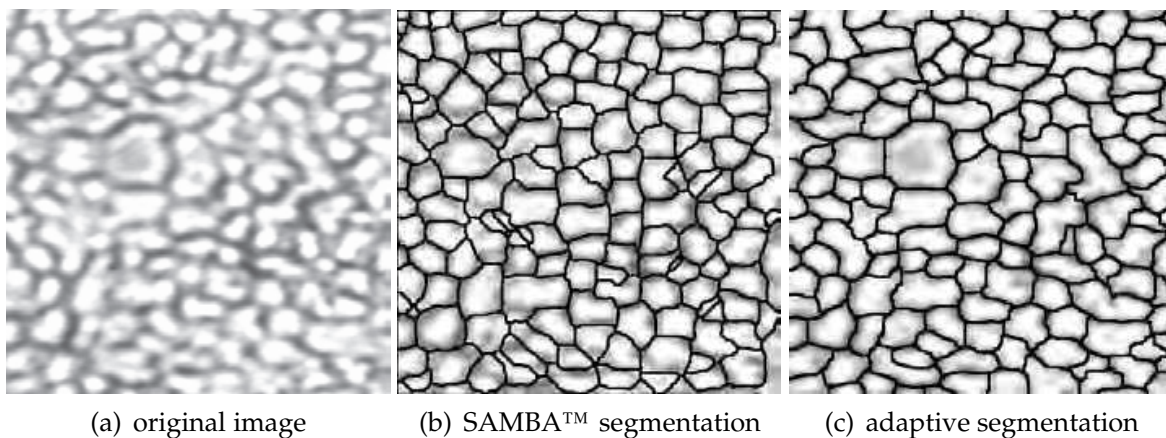


Fig. 11. Image segmentation of human endothelial cornea cells (a). The process achieved by the GANIP-based morphological approach (c) provides better results (visually and from the point of view of ophthalmologists) than the SAMBA™ software (Gain et al., 2002) (b).

The detection process achieved by the GANIP-based morphological approach provides better results (from the point of view of the ophthalmologists) than the SAMBA™ software. Those results highlight the spatially-variant adaptivity of the GANIP-based operators.

4. Conclusion and prospects

The General Adaptive Neighborhood Image Processing (GANIP) approach allows efficient gray-tone image processing operators to be built. Those GAN-based operators are fully adaptive and enable to process an image in a consistent way with the image formation model, while preserving its regions without damaging its transitions. The theoretical aspects have been practically highlighted on real biomedical application examples (ophtalmology, microbiology, neurology, proteome biology) by using several image processing techniques in various biomedical fields, namely image restoration, enhancement and segmentation.

Different scales of biomedical structures have been investigated (proteins, cells, organs, tissues) with a resolution ranging from nanometres to centimetres.

In its current state of progress, the GANIP approach only deals with image transformations as well in image processing as in image analysis. Novel GANIP-based image processing techniques have been recently proposed by the authors (Debayle & Pinoli, 2011). Image quantitative analysis now appears clearly as a strong need. Therefore, the authors are currently working on combining geometric measurement concepts with GANIP (Rivollier et al., 2009; 2010d). Indeed, in the GANIP image representation an image is described in terms of particular subsets within the spatial support: the GANs. Thus, topological, geometrical and morphological measurements (Rivollier et al., 2010a;b;c) can be applied to the GANs associated to a given image. In this way, a local adaptive geometric quantitative analysis can be performed on gray-tone images without a segmentation step, classically required in image analysis.

5. Acknowledgments

The authors would like to thank the different partners from the University Hospital Center of Saint-Etienne and from the LPMG CNRS Unit in France who have kindly supplied different original images studied in this paper.

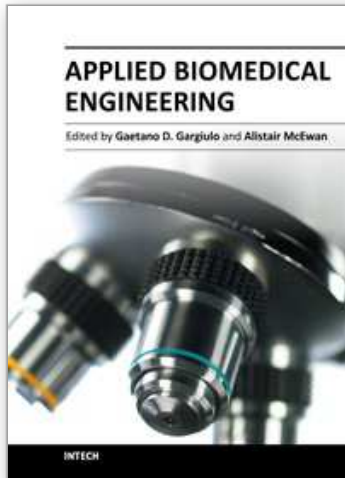
6. References

- Amattouch, M. (2005). *Théorie de la Mesure et Analyse d'Image*, Master's thesis, Ecole Nationale Supérieure des Mines, Saint-Etienne, France.
- Bernard, F. (2008). *IDADIGE : Procédé de traitement des images de gels électrophorèse bidimensionnelle différentielle dans le contexte de la recherche de marqueurs protéiques*, PhD thesis, Ecole Nationale Supérieure des Mines, Saint-Etienne, France.
- Beucher, S. & Lantuejoul, C. (1979). Use of watersheds in contour detection, *International Workshop on Image Processing, Real-Time Edge and Motion Detection/Estimation*, Rennes, France.
- Bouannaya, N. & Schonfeld, D. (2008). Theoretical Foundations of Spatially-Variant Mathematical Morphology Part II: Gray-Level Images, *IEEE Transactions on Pattern Analysis and Machine Intelligence* 30(5): 837–850.
- Choquet, G. (2000). *Cours de Topologie*, Dunod, Paris, France, chapter Espaces topologiques et espaces métriques, pp. 45–51.
- Ciuc, M., Rangayyan, R. M., Zaharia, T. & Buzuloiu, V. (2000). Filtering Noise in Color Images using Adaptive-Neighborhood Statistics, *Electronic Imaging* 9(4): 484–494.
- Debayle, J. & Pinoli, J. C. (2005a). Multiscale Image Filtering and Segmentation by means of Adaptive Neighborhood Mathematical Morphology, *IEEE International Conference on Image Processing*, Vol. 3, Genova, Italy, pp. 537–540.
- Debayle, J. & Pinoli, J. C. (2005b). Spatially Adaptive Morphological Image Filtering using Intrinsic Structuring Elements, *Image Analysis and Stereology* 24(3): 145–158.
- Debayle, J. & Pinoli, J. C. (2006a). General Adaptive Neighborhood Image Processing - Part I: Introduction and Theoretical Aspects, *Journal of Mathematical Imaging and Vision* 25(2): 245–266.
- Debayle, J. & Pinoli, J. C. (2006b). General Adaptive Neighborhood Image Processing - Part II: Practical Application Examples, *Journal of Mathematical Imaging and Vision* 25(2): 267–284.

- Debayle, J. & Pinoli, J. C. (2009a). General Adaptive Neighborhood Choquet Image Filtering, *Journal of Mathematical Imaging and Vision* 35(3): 173–185.
- Debayle, J. & Pinoli, J. C. (2009b). General Adaptive Neighborhood Representation for Adaptive Choquet Image Filtering, *10th European Congress of Stereology and Image Analysis*, Milan, Italy, pp. 431–436.
- Debayle, J. & Pinoli, J. C. (2011). General Adaptive Neighborhood-Based Pretopological Image Filtering, *Journal of Mathematical Imaging and Vision* . In Press.
- Gain, P., Thuret, G., Kodjikian, L., Gavet, Y., Turc, P. H., Theillere, C., Acquart, S., LePetit, J. C., Maugery, J. & Campos, L. (2002). Automated Tri-Image Analysis of Stored Corneal Endothelium, *British Journal of Ophthalmology* 86: 801–808.
- Gavet, Y. & Pinoli, J. C. (2008). Visual Perception based Automatic Recognition of Cell Mosaics in Human Corneal Endothelium Microscopy Images, *Image Analysis and Stereology* 27: 53–61.
- Gonzalez, R. C. & Woods, R. E. (2008). *Digital Image Processing*, third edn, Prentice Hall.
- Gordon, R. & Rangayyan, R. M. (1984). Feature Enhancement of Mammograms using Fixed and Adaptive Neighborhoods, *Applied Optics* 23(4): 560–564.
- Grabisch, M. (1994). Fuzzy Integrals as a Generalized Class of Order Filters, *Proc. of the SPIE*, Vol. 2315, pp. 128–136.
- Jourlin, M. & Pinoli, J. C. (1988). A Model for Logarithmic Image Processing, *Journal of Microscopy* 149: 21–35.
- Jourlin, M. & Pinoli, J. C. (2001). Logarithmic Image Processing : The Mathematical and Physical Framework for the Representation and Processing of Transmitted Images, *Advances in Imaging and Electron Physics* 115: 129–196.
- Jourlin, M., Pinoli, J. C. & Zeboudj, R. (1988). Contrast Definition and Contour Detection for Logarithmic Images, *Journal of Microscopy* 156: 33–40.
- Maragos, P. & Vachier, C. (2009). Overview of Adaptive Morphology: Trends and Perspectives, *IEEE International Conference on Image Processing*, Cairo, Egypt, pp. 2241–2244.
- Matheron, G. (1967). *Eléments pour une Théorie des Milieux Poreux*, Masson, Paris, France.
- Murofushi, T. & Sugeno, M. (1989). An Interpretation of Fuzzy Measure and the Choquet Integral as an Integral with respect to a Fuzzy Measure, *Fuzzy Sets and Systems* 29: 201–227.
- Oppenheim, A. V. (1967). Generalized Superposition, *Information and Control* 11: 528–536.
- Pinoli, J. C. (1987). *Contribution à la Modélisation, au Traitement et à l'Analyse d'Image*, PhD thesis, Department of Mathematics, University of Saint-Etienne, France.
- Pinoli, J. C. (1991). A Contrast Definition for Logarithmic Images in the Continuous Setting, *Acta Stereologica* 10: 85–96.
- Pinoli, J. C. (1997a). A General Comparative Study of the Multiplicative Homomorphic, Log-Ratio and Logarithmic Image Processing Approaches, *Signal Processing* 58: 11–45.
- Pinoli, J. C. (1997b). The Logarithmic Image Processing Model : Connections with Human Brightness Perception and Contrast Estimators, *Journal of Mathematical Imaging and Vision* 7(4): 341–358.
- Pinoli, J. C. & Debayle, J. (2007). Logarithmic Adaptive Neighborhood Image Processing (LANIP): Introduction, Connections to Human Brightness Perception and Application Issues, *Journal on Advances in Signal Processing - Special issue on Image Perception* 2007: Article ID 36105, 22 pages.

- Pinoli, J. C. & Debayle, J. (2009). General Adaptive Neighborhood Mathematical Morphology, *IEEE International Conference on Image Processing*, Cairo, Egypt, pp. 2249–2252.
- Ramponi, G., Strobel, N., Mitra, S. K. & Yu, T. H. (1996). Nonlinear Unsharp Masking Methods for Image-Contrast Enhancement, *Journal of Electronic Imaging* 5(3): 353–366.
- Rivollier, S., Debayle, J. & Pinoli, J. C. (2010a). Shape diagrams for 2D compact sets - Part I: analytic convex sets, *Australian Journal of Mathematical Analysis and Applications* 7(2-3): 1–27.
- Rivollier, S., Debayle, J. & Pinoli, J. C. (2010b). Shape diagrams for 2D compact sets - Part II: analytic simply connected sets, *Australian Journal of Mathematical Analysis and Applications* 7(2-4): 1–21.
- Rivollier, S., Debayle, J. & Pinoli, J. C. (2010c). Shape diagrams for 2D compact sets - Part III: convexity discrimination for analytic and discretized simply connected sets, *Australian Journal of Mathematical Analysis and Applications* 7(2-5): 1–18.
- Rivollier, S., Debayle, J. & Pinoli, J. C. (2009). General Adaptive Neighborhood-Based Minkowski Maps for Gray-Tone Image Analysis, *10th European Congress of Stereology and Image Analysis*, Milan, Italy, pp. 219–224.
- Rivollier, S., Debayle, J. & Pinoli, J. C. (2010d). Integral geometry and general adaptive neighborhood for multiscale image analysis, *International Journal of Signal and Image Processing* 1(3): 141–150.
- Roerdink, J. B. T. M. (2009). Adaptivity and group invariance in mathematical morphology, *IEEE International Conference on Image Processing*, Cairo, Egypt, pp. 2253–2256.
- Rosenfeld, A. (1969). *Picture Processing by Computers*, Academic Press, New-York, U.S.A.
- Salembier, P. (1992). Structuring Element Adaptation for Morphological Filters, *Journal of Visual Communication and Image Representation* 3(2): 115–136.
- Serra, J. (1982). *Image Analysis and Mathematical Morphology*, Academic Press, London, U.K.
- Soille, P. (2003). *Morphological Image Analysis. Principles and Applications*, Springer Verlag, New York, U.S.A.
- Stockham, T. G. (1972). Image Processing in the Context of a Visual Model, *Proc. of the IEEE*, Vol. 60, pp. 825–842.
- Sugeno, M. (1974). *Theory of Fuzzy Integrals and its Applications*, PhD thesis, Tokyo Institute of Technology, Japan.

IntechOpen



Applied Biomedical Engineering

Edited by Dr. Gaetano Gargiulo

ISBN 978-953-307-256-2

Hard cover, 500 pages

Publisher InTech

Published online 23, August, 2011

Published in print edition August, 2011

This book presents a collection of recent and extended academic works in selected topics of biomedical technology, biomedical instrumentations, biomedical signal processing and bio-imaging. This wide range of topics provide a valuable update to researchers in the multidisciplinary area of biomedical engineering and an interesting introduction for engineers new to the area. The techniques covered include modelling, experimentation and discussion with the application areas ranging from bio-sensors development to neurophysiology, telemedicine and biomedical signal classification.

How to reference

In order to correctly reference this scholarly work, feel free to copy and paste the following:

Johan Debayle and Jean-Charles Pinoli (2011). General Adaptive Neighborhood Image Processing for Biomedical Applications, Applied Biomedical Engineering, Dr. Gaetano Gargiulo (Ed.), ISBN: 978-953-307-256-2, InTech, Available from: <http://www.intechopen.com/books/applied-biomedical-engineering/general-adaptive-neighborhood-image-processing-for-biomedical-applications>

INTECH
open science | open minds

InTech Europe

University Campus STeP Ri
Slavka Krautzeka 83/A
51000 Rijeka, Croatia
Phone: +385 (51) 770 447
Fax: +385 (51) 686 166
www.intechopen.com

InTech China

Unit 405, Office Block, Hotel Equatorial Shanghai
No.65, Yan An Road (West), Shanghai, 200040, China
中国上海市延安西路65号上海国际贵都大饭店办公楼405单元
Phone: +86-21-62489820
Fax: +86-21-62489821

© 2011 The Author(s). Licensee IntechOpen. This chapter is distributed under the terms of the [Creative Commons Attribution-NonCommercial-ShareAlike-3.0 License](#), which permits use, distribution and reproduction for non-commercial purposes, provided the original is properly cited and derivative works building on this content are distributed under the same license.

IntechOpen

IntechOpen